Supporting Information

Mussel-Inspired Catechol-Formaldehyde Resin Coated Fe_3O_4 Core-Shell Magnetic Nanospheres: An Effective Catalyst Support for Highly Active Palladium Nanoparticles

Yanan Zhang, Yu Yang, Haichao Duan and Changli Lü*

College of Chemistry, Northeast Normal University, Changchun 130024, P. R. China

E-mail addresses: lucl055@nenu.edu.cn (C. Lü).

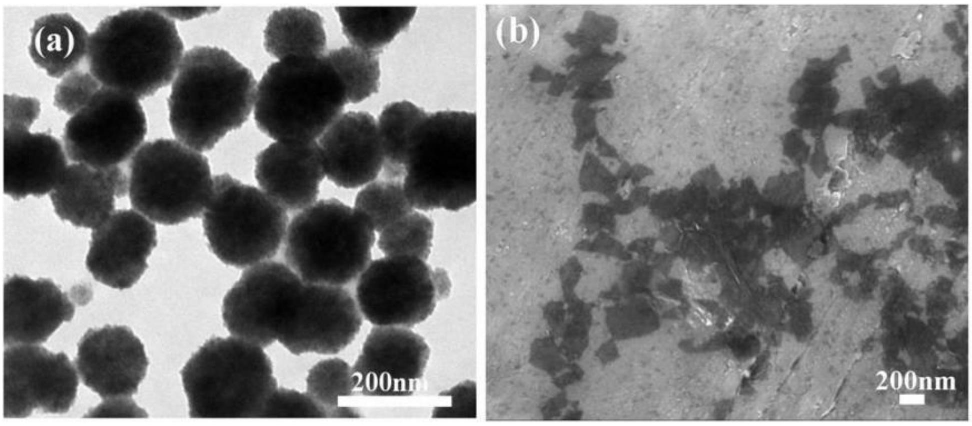

Figure S1. TEM images of (a) Fe_3O_4 nanoparticles and (b) graphene oxide sheets.

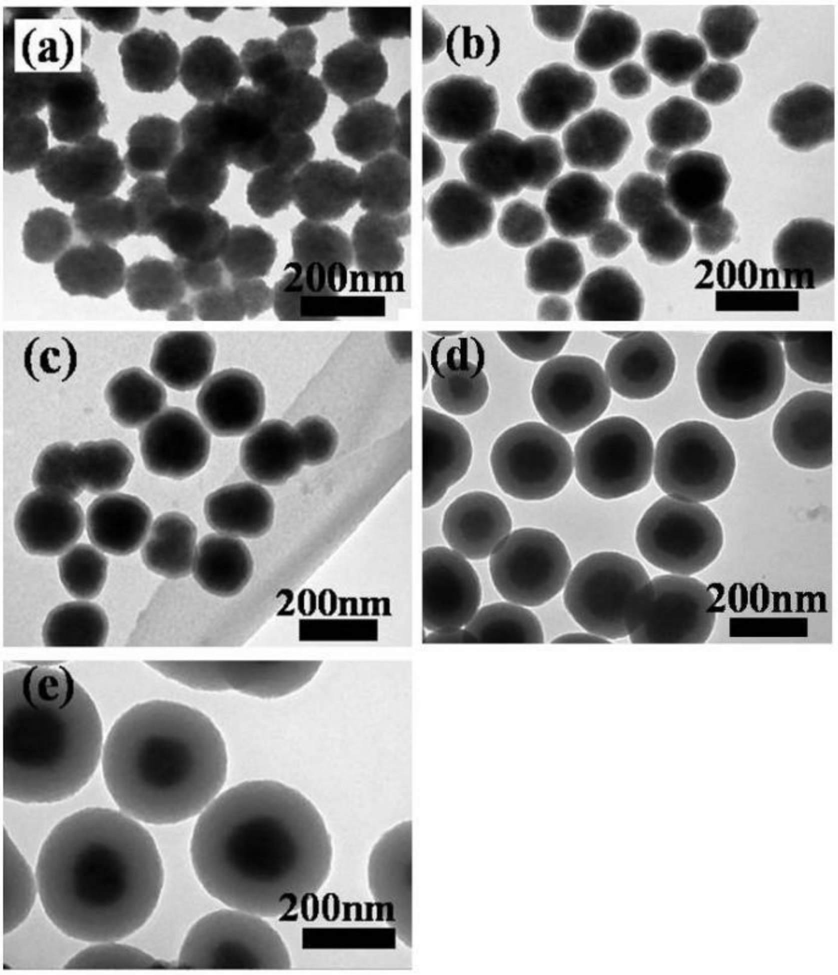

Figure S2. TEM images of Fe_3O_4@CFR core-shell nanospheres obtained from different amounts of catechol: (a) 0.01 g, (b) 0.02 g, (c) 0.04 g, (d) 0.08 g, (e) 0.16 g. Reaction conditions: formaldehyde solution 0.07 mL, Fe_3O_4 15.0 mg, water 20 mL, ammonia solution 0.075 mL, heating time 100 min, and reaction temperature 160 °C.

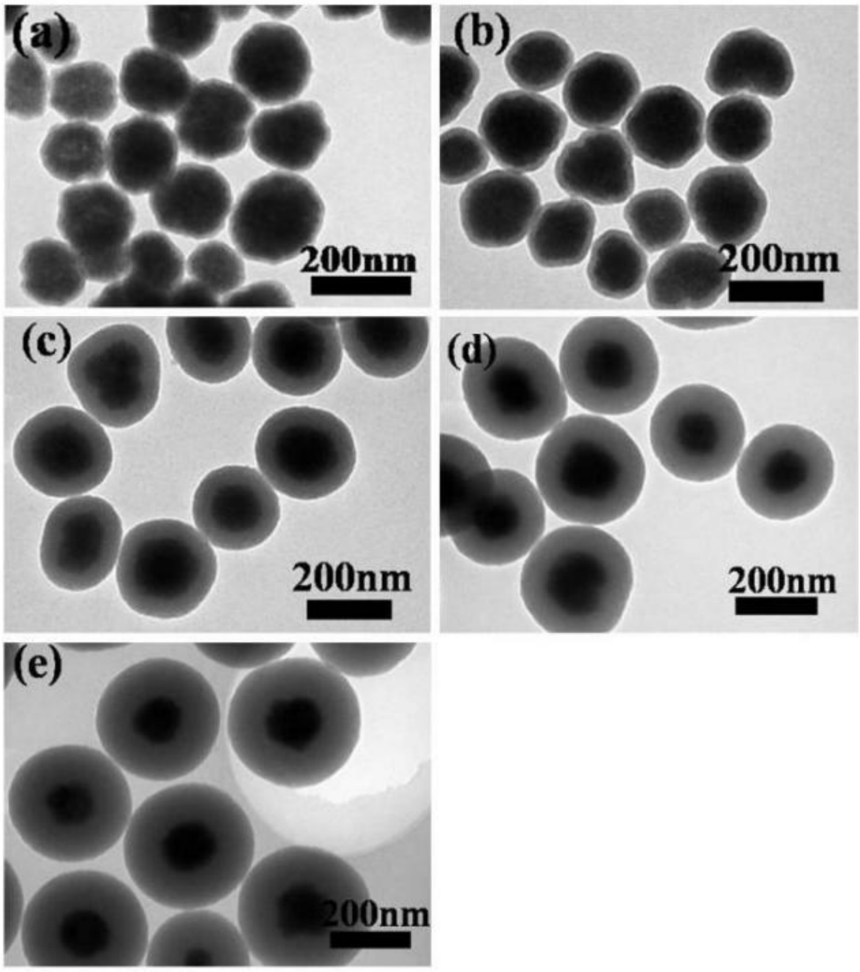

Figure S3. TEM images of Fe_3O_4@CFR core-shell nanospheres prepared with different amounts of formaldehyde solution: (a) 0.01 mL, (b) 0.035 mL, (c) 0.07 mL, (d) 0.105 mL, and (e) 0.14 mL. Reaction conditions: catechol 0.1 g, Fe_3O_4 15.0 mg, water 20 mL, ammonia solution 0.075 mL, heating time 100 min, and reaction temperature 160 °C.

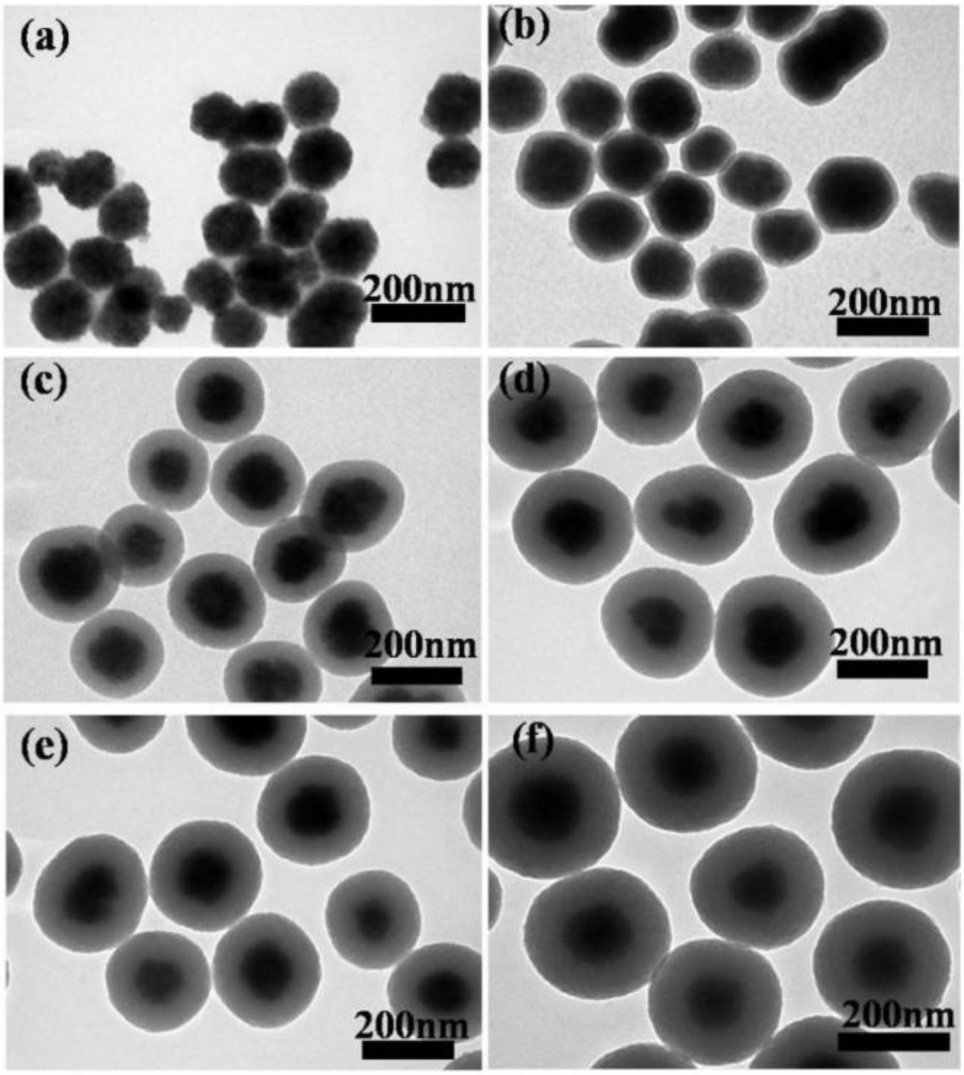

Figure S4. TEM images of Fe_3O_4@CFR core-shell nanospheres prepared with different reaction temperatures: (a) 80 °C, (b) 100 °C, (c) 120 °C, (d) 140 °C, (e) 160 °C, and (f) 180 °C. Reaction conditions: formaldehyde solution 0.14 mL, catechol 0.1 g, Fe_3O_4 15.0 mg, water 20 mL, ammonia solution 0.075 mL, heating time 100 min.

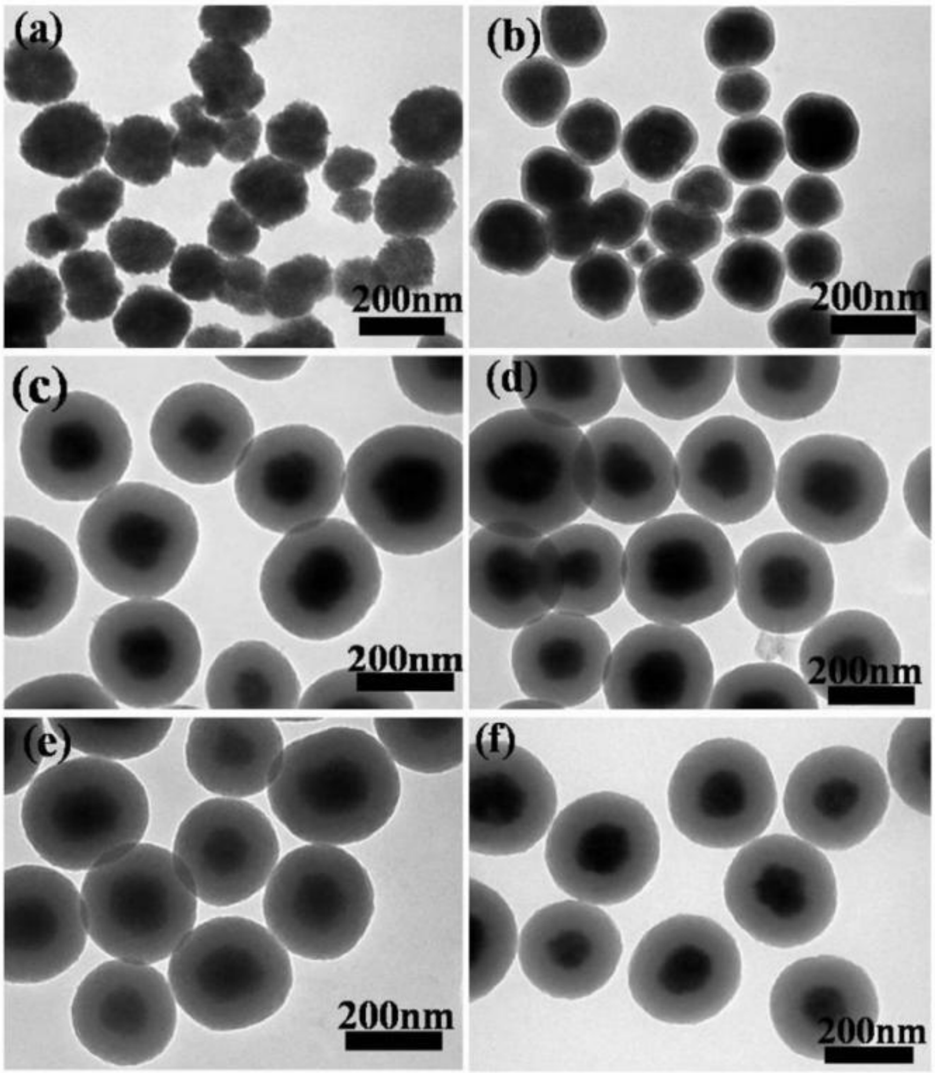

Figure S5. TEM images of theFe$_3$O$_4$@CFR core-shell nanospheres prepared with different reaction times: (a) 20 min, (b) 40 min, (c) 60 min, (d) 80 min, (e) 100 min, and (f) 120 min. Reaction conditions: formaldehyde solution 0.14ml, catechol 0.1g, Fe$_3$O$_4$ 15.0 mg, water 20 mL, ammonia solution 0.075 mL, and reaction temperature 160 °C.

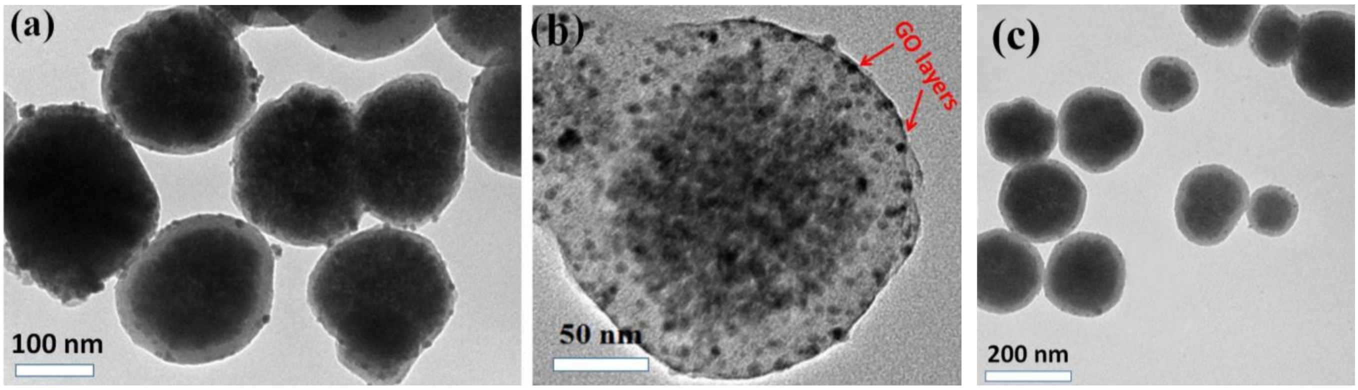

Figure S6. (a) Low-magnification and (b) High-magnification TEM images of Fe_3O_4@CFR@GO@PdNPs nanospheres. (c). Low-magnification TEM image of Fe_3O_4@CFR@PdNPs nanospheres.

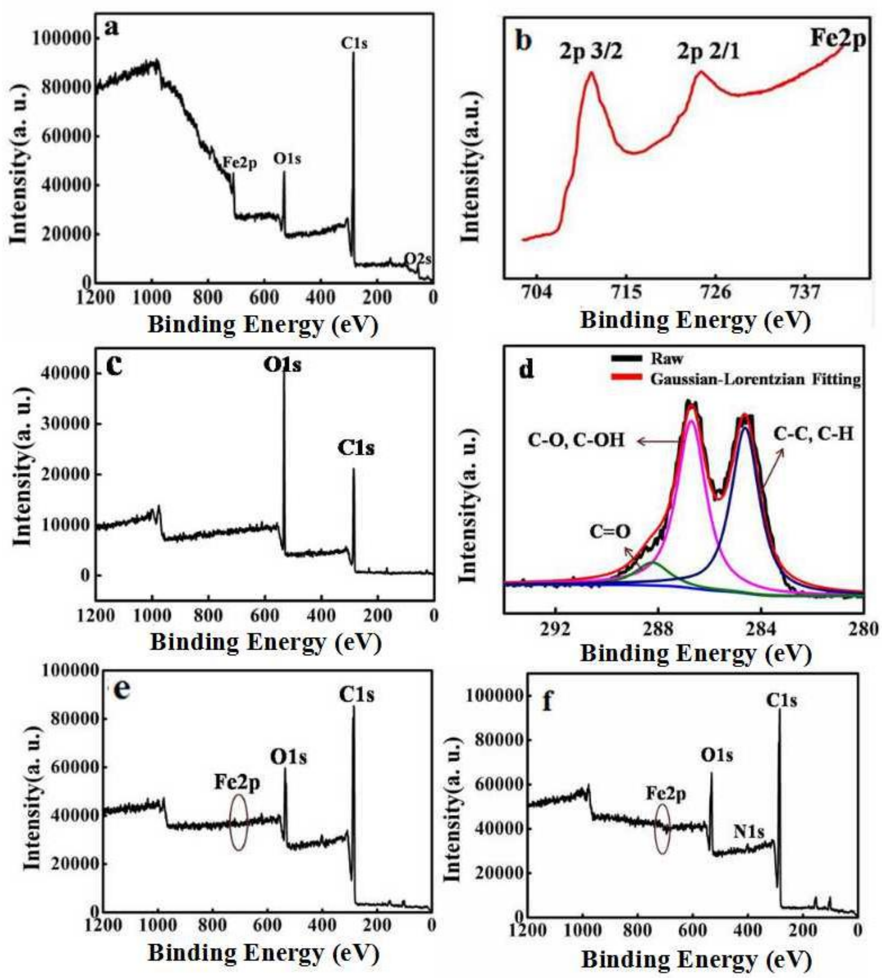

Figure S7. XPS survey spectra of (a) Fe_3O_4 NPs, (c) GO, (e) Fe_3O_4@CFR and (f) Fe_3O_4@CFR@GO nanospheres. High-resolution XPS spectra of (b) Fe2p for Fe_3O_4 NPs and (d) C1s for GO.

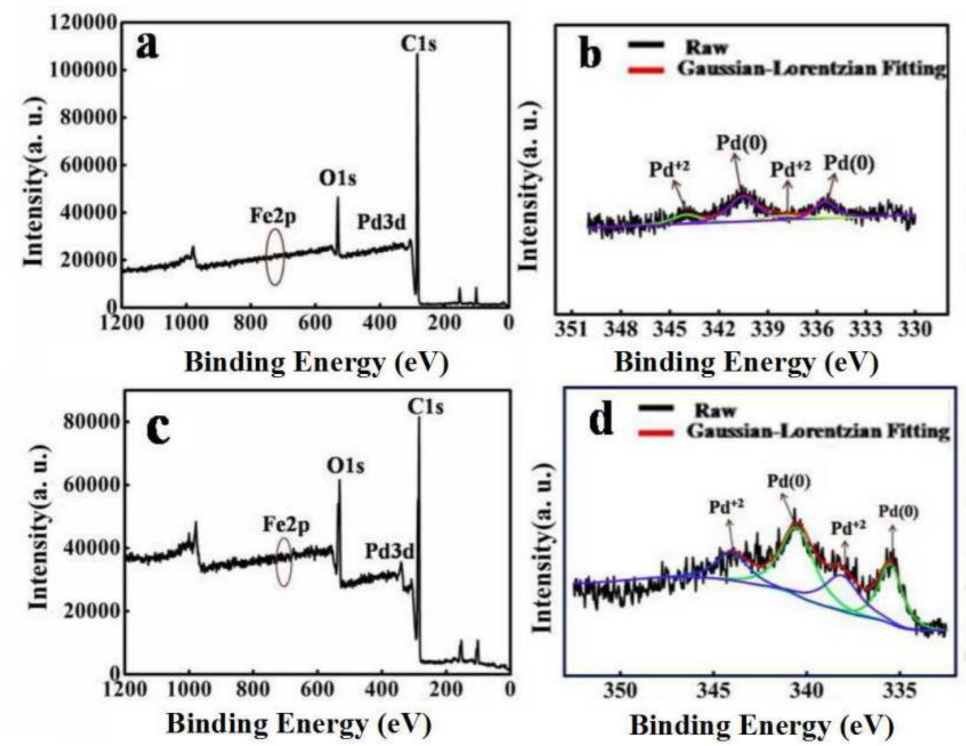

Figure S8. XPS spectra of (a,b) Fe_3O_4@CFR@PdNPs and (c,d) Fe_3O_4@CFR@GO@PdNPs nanospheres (a,c: survey spectra, b,d: High-resolution Pd2p spectra).

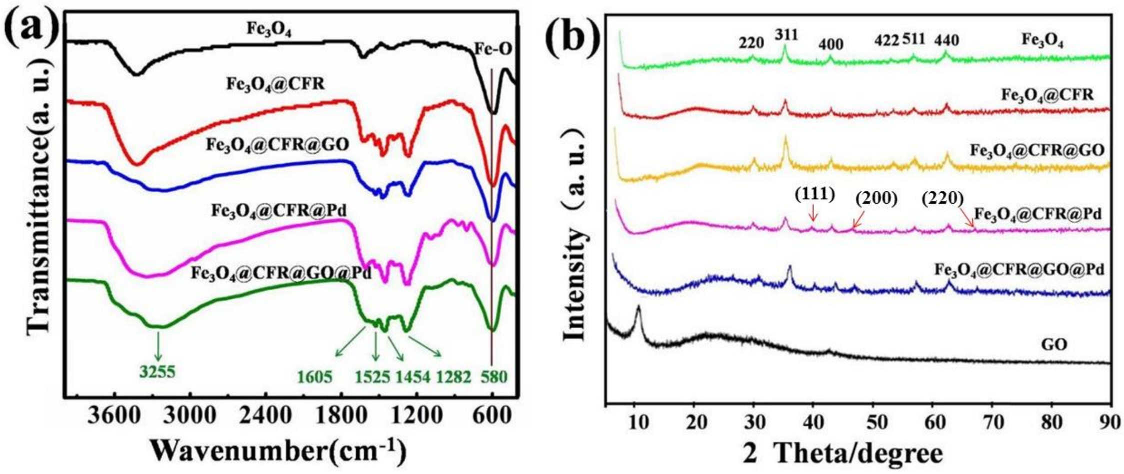

Figure S9. (a) FTIR and (b) XRD spectra of different samples.

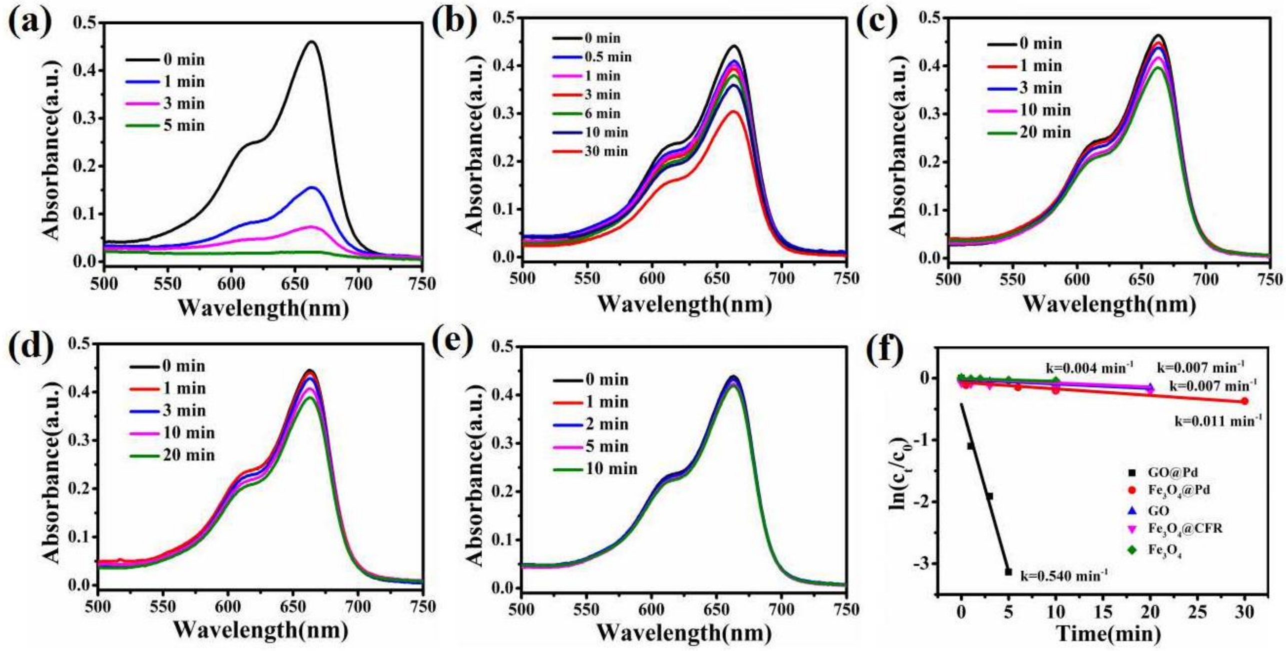

Figure S10. Successive reduction reaction of MB using catalysts (20 μL): (a) GO@Pd, (b) Fe_3O_4@Pd, (c) GO, (d) Fe_3O_4@CFR, (e) Fe_3O_4 and (f) Plots of ln (c_t /c_0) vs. reaction time (t) for different control catalysts (0.05 mg mL^{-1} catalyst, 2.0 mL of 5 mg L^{-1} MB and 1.0 mL of 0.5 M $NaBH_4$ were used for the reduction of MB).

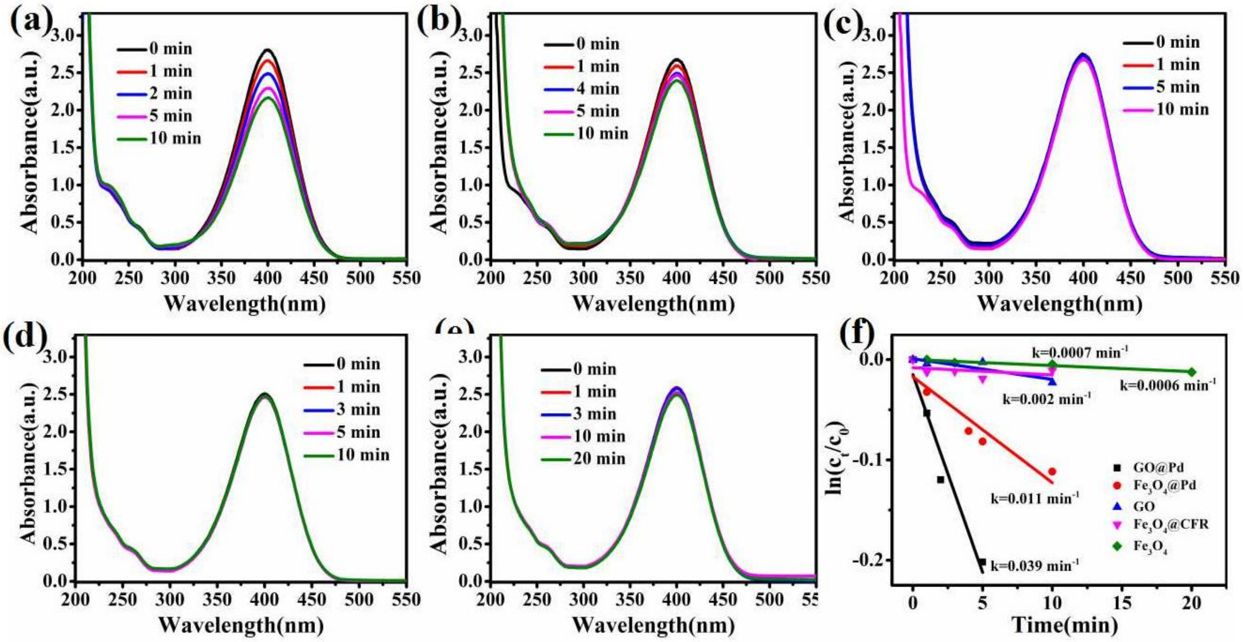

Figure S11. Successive reduction of *p*-NP using (a) GO@Pd, (b) Fe_3O_4@Pd, (c) GO, (d) Fe_3O_4@CFR, (e) Fe_3O_4 and (f) Plots of ln (c_t /c_0) vs. reaction time (t) for different control catalysts (0.05 mg mL^{-1} catalyst, 2.0 mL of 0.16 mM *p*-NP and 1.0 mL of 0.2 M $NaBH_4$ were used for the reduction of *p*-NP).

Table S1. Properties and Synthesis Parameters of Fe_3O_4@CFR Core-shell Nanospheres.

sample		Fe_3O_4 (g)	catechol (g)	formaldehyde solution (mL)	NH_3H_2O (mL)	water (mL)	temperature (℃)	time (min)	shell size (nm)
CFR-1	Effect of catechol and formaldehyde	0.015	0.01	0.014	0.075	20	160	100	0
CFR-2		0.015	0.025	0.035	0.075	20	160	100	9±3
CFR-3		0.015	0.05	0.07	0.075	20	160	100	35±4
CFR-4		0.015	0.1	0.14	0.075	20	160	100	65±3
CFR-5		0.015	0.125	0.179	0.075	20	160	100	119±5
CFR-6		0.015	0.15	0.21	0.075	20	160	100	170±8
CFR-7	Effect of catechol	0.015	0.01	0.07	0.075	20	160	100	0
CFR-8		0.015	0.02	0.07	0.075	20	160	100	9±1
CFR-9		0.015	0.04	0.07	0.075	20	160	100	21±2
CFR-10		0.015	0.08	0.07	0.075	20	160	100	47±3
CFR-11		0.015	0.16	0.07	0.075	20	160	100	76±7
CFR-12	Effect of formaldehyde	0.015	0.05	0.01	0.075	20	160	100	8±2
CFR-13		0.015	0.05	0.035	0.075	20	160	100	14±3
CFR-14		0.015	0.05	0.07	0.075	20	160	100	35±4
CFR-15		0.015	0.05	0.105	0.075	20	160	100	71±3
CFR-16		0.015	0.05	0.14	0.075	20	160	100	99±4
CFR-17	Effect of temperature	0.015	0.1	0.14	0.075	20	80	100	0
CFR-18		0.015	0.1	0.14	0.075	20	100	100	15±3
CFR-19		0.015	0.1	0.14	0.075	20	120	100	39±4
CFR-20		0.015	0.1	0.14	0.075	20	140	100	62±3
CFR-21		0.015	0.1	0.14	0.075	20	160	100	65±3
CFR-22		0.015	0.1	0.14	0.075	20	180	100	68±4
CFR-23	Effect of time	0.015	0.1	0.14	0.075	20	160	20	0
CFR-24		0.015	0.1	0.14	0.075	20	160	40	12±2
CFR-25		0.015	0.1	0.14	0.075	20	160	60	57±5
CFR-26		0.015	0.1	0.14	0.075	20	160	80	62±3
CFR-27		0.015	0.1	0.14	0.075	20	160	100	65±3
CFR-28		0.015	0.1	0.14	0.075	20	160	120	66±4

Table S2. Comparison of the Ability of Various Catalysts for Catalyzing the Reduction of MB.

samples	time (s) [a]	k (min^{-1}) [b]	TOF (min^{-1}) [c]	references
Fe_3O_4@C_{16}@CTS-Au NPs	43200	1.8	1.91	1
Pd-TNPs/RGO	420	0.4	1.226	2
Ag/MFC	600	0.34	-	3
graphene-PDA-Pd	300	0.1224	-	4
AgNPs-Fe_3O_4@PDA	1800	0.0864	-	5
Fe_3O_4@PDA-Ag	540	0.43	-	6
Fe_3O_4@(A–V)-silica–Pd	＞1200	0.079	-	7
Pd NPs (pc-7)	420	1.006	108.27	8
Pd-PIBrGO	30	9.563	2198.4	9
Pd/Fe_3O_4@-AlOOH-YSMs	83	3.06	-	10
Mesoporous 3D wood@Pd membrane	Rapidly	-	2.02	11
MpSi-Pd	4	0.655	1.77	12
Pd55DENs (dendrimer, G-5 PAMAM-OH)	25	23.38	-	13
Fe_3O_4@CFR@PdNPs	30	14.07	3156	This work
Fe_3O_4@CFR@GO@PdNPs	15	23.58	5260	This work

[a] The reduction time of MB in the presence of catalyst. [b]Apparent rate constant. [c] Turnover frequency (TOF), defined as moles of MB molecules reduced per mole of Pd catalyst per unit time, is calculated based on the Pd contents in Fe_3O_4@CFR@GO@ PdNPs (2.2 wt%) and Fe_3O_4@CFR@PdNPs (1.9 wt%) determined by ICP.

Table S3. Comparison of the Ability of Reported Various Catalysts for Suzuki Cross-Coupling Reactions of Bromobenzene and Phenylboronic Acid.

samples	support materials	reaction conditions	conversion (%)	references
PS@RGO@Pd	PS@RGO	0.2 mol % Pd, base: K_2CO_3, solvent: EtOH / H_2O, T = RT, t= 10 h	95	14
Pd/Fe_3O_4@SiO_2@KCC-1	Fe_3O_4@SiO_2@KCC-1	0.2 mol % Pd, base: K_2CO_3, solvent: EtOH, T = 80 ºC, t = 6 h	90.8	15
PFG-Pd	PFG	1.2 mol % Pd, base: K_2CO_3, solvent: H_2O / EtOH = 1:1, T = 80 º C, t = 10 h	95	16
Pd@PN-CeO_2	PN-CeO_2	0.14 mol % Pd, base: K_2CO_3, solvent: DMF / H_2O = 1:1, T = 90 ºC, t = 1 h	99.1	17
Pd@CD–GNS	CD-GNS	0.2 mol % Pd, base: Na_2CO_3, solvent: H_2O, T = 90 ºC, t = 3 h	93	18
$Ni_{0.20}Pd_{0.05}$/CB	Carbon black (CB)	0.1 mol % Pd, base: K_2CO_3, solvent: H_2O, T = 30º C, t = 4 h	14	19
Pd NPs/CNFs	Carbon nanofibers (CNFs)	0.22 mol % Pd, base: K_2CO_3, solvent: EtOH / H_2O = 8:6, T = 80 ºC, t = 4 h	25	20
Fe_3O_4-DA-DMG/Pd^0	Fe_3O_4-DA-DMG	0.1 mol % Pd, base: K_2CO_3, solvent: H_2O, T = 80 ºC, t = 12 h	97.4	21
Pd-Fe_3O_4/rGO	Fe_3O_4/rGO	0.25 mol % Pd, base: K_2CO_3, solvent: EtOH / H_2O = 1:1, T = 80 ºC, t = 1 h	94	22
Pd-P(Ss-DVB) spheres	P(Ss-DVB) spheres	0.5 mol % Pd, base: Na_2CO_3, solvent: DMF / H_2O = 1:1, T = 100 º C; t = 12 h	80	23
Pd@CzMOP	CzMOP	0.2 mol % Pd, base: K_2CO_3, solvent: DMF, T = 80 º C, t = 6 h	90	24
Si-IL@Pd(0) NPs	Click ionic-silica	0.1 mol % Pd, base: K_2CO_3, solvent: H_2O, T= 50 ºC, t = 4 h	55	25
Im–Phos–SiO_2@Fe_3O_4@Pd	Im–Phos-SiO_2@Fe_3O_4	0.3 mol % Pd, base: K_2CO_3, solvent: EtOH / H_2O = 1:1, T= 60º C, t = 18 h	90	26
Fe_3O_4@CFR@GO@PdNPs	Fe_3O_4@CFR@GO	0.14 mol % Pd, base: K_2CO_3, solvent: H_2O, T = RT, t = 24 h, or 80 º C, t = 2 h	99.2	This work

Table S4. Substrate Study for the Fe_3O_4@CFR@GO@PdNPs-Catalyzed Suzuki Cross-Coupling Reaction.[a]

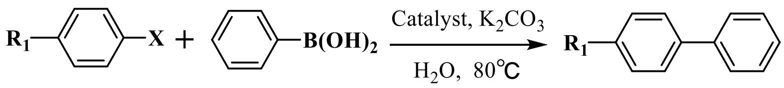

entry	R_1	X	catalyst	time (h)	conversion (%) [b]
1	H	Cl	Fe_3O_4@CFR@GO@Pd	2	99.1
2	4-CH_3	Cl	Fe_3O_4@CFR@GO@Pd	2	89.7
3	4-OCH_3	Cl	Fe_3O_4@CFR@GO@Pd	2	92.8
4	H	Br	Fe_3O_4@CFR@GO@Pd	2	99.2
5	4-CH_3	Br	Fe_3O_4@CFR@GO@Pd	2	94.7
6	4-OCH_3	Br	Fe_3O_4@CFR@GO@Pd	2	88.5
7	4-CN	Br	Fe_3O_4@CFR@GO@Pd	2	99.1
8	4-CHO	Br	Fe_3O_4@CFR@GO@Pd	2	99.9
9	H	I	Fe_3O_4@CFR@GO@Pd	2	99.5
10	4-CH_3	I	Fe_3O_4@CFR@GO@Pd	2	95.6
11	4-OCH_3	I	Fe_3O_4@CFR@GO@Pd	2	93.2
12	4-CN	I	Fe_3O_4@CFR@GO@Pd	2	99.7

[a] Reaction condition: aryl halide (0.5 mmol), phenylboronic (0.6 mmol), K_2CO_3 (1.5 mmol), water (5.0 mL), Fe_3O_4@CFR@GO@Pd catalyst (0.14 mol% Pd). [b] Conversion was determined by GC analysis.

Table S5. Comparative Study of Different Catalysts for Suzuki Cross-Coupling Reactions of Bromobenzene and Phenylboronic Acid.[a]

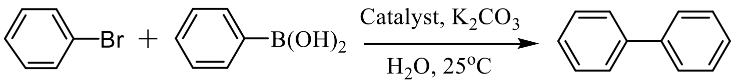

entry	catalyst	time (h)	conversion (%) [b]
1	Fe_3O_4@CFR@GO@Pd (0.14 mol% Pd)	24	99.2
2	Fe_3O_4@CFR@Pd (0.14 mol% Pd)	24	91.6
3	GO@Pd (0.14 mol% Pd)	24	62.0
4	Fe_3O_4@Pd (0.14 mol% Pd)	24	55.9
5	Fe_3O_4@CFR (7.0 mg)	24	undetectable
6	Fe_3O_4 (7.0 mg)	24	undetectable
7	GO (7.0 mg)	24	undetectable

[a] Reaction condition: bromobenzene (0.5 mmol), phenylboronic (0.6 mmol), K_2CO_3 (1.5 mmol), water (5.0 mL). [b] Conversion was determined by GC analysis.

Table S6. Comparison of the Ability of Various Catalysts for the Reduction of 4-NP.

samples	support materials	*k* (min^{-1})	TOF(h^{-1}) [a]	references
Au-PDA/RGO	PDA/RGO	0.012	42	27
GO/TWEEN 20-Au	GO/TWEEN 20	0.2537	126	28
Ag-Au-rGO	rGO	0.2082	152	29
Au NPs@GFDP	GFDP	0.665	439	30
PS@RGO@Pd	PS@RGO	0.286	-	14
Pd/Fe_3O_4@SiO_2@KCC-1	Fe_3O_4@SiO_2@KCC-1	1.176	-	15
CMF@PDA/Pd	CMF@PDA	-	1.594	31
Pd/Fe_3O_4@-AlOOH-YSMs	Fe_3O_4@-AlOOH-YSMs	2.22	-	10
C_3N_4@Pd	C_3N_4	0.15	-	32
MpSi-Pd	Magnetic porous Si	0.159	85.1	12
Pd/CNs	Cellulose nanocrystal	0.342	879.4	33
Fe_3O_4@CFR@PdNPs	Fe_3O_4@CFR	0.956	2800	This work
Fe_3O_4@CFR@GO@PdNPs	Fe_3O_4@CFR@GO	2.458	6720	This work

[a] Turnover frequency (TOF) is defined as the number of moles of 4-NP reduced per mole of Pd catalyst per hour.

Calculation method of TOF:

The TOF values of the catalytic reactions for MB were calculated according to the following equation:[34]

$$TOF = \frac{[MB] \times conversion}{[Pd] \times t} \tag{1}$$

The molar concentration [MB] of substrate was fixed to be 1.04×10^{-5} M. The Pd molar concentration [Pd] of both Fe_3O_4@CFR@GO@PdNPs and Fe_3O_4@CFR@PdNPs in catalytic systems was calculated to be 1.98×10^{-8} M by ICP-AES results. The conversion at reaction time t can be obtained from Figure 4a-c. We estimated the TOF values for all the runs with the conversion of MB at 50%.

The TOF values of the catalytic reactions for 4-nitrophenol were calculated according to the equation similar to MB. The molar concentration [4-NP] of substrate was 1.0×10^{-4} M. The Pd molar concentration [Pd] of both Fe_3O_4@CFR@GO@PdNPs and Fe_3O_4@CFR@PdNPs in reaction systems was calculated to be 1.78×10^{-7} M by ICP-AES results. The conversion at reaction time t can be obtained from Figure 6a and b. The calculation for TOF values of the catalytic reduction of nitrophenols with the conversion of NPs at 100%.

REFERENCES

(1) Hua, J.; Dong, Y. L.; Rahman, Z.; Ma, Y. H.; Ren, C. L.; Che, X. G. In Situ Preparation of Core-Satellites Nanostructural Magnetic-Au NPs Composite for Catalytic Degradation of Organic Contaminants. *Chem. Eng. J.* 2**014**, *254*, 514–523.

(2) Fu, G. T.; Tao, L.; Zhang, M.; Chen, Y.; Tang, Y. W.; Lin, J.; Lu, T. H. One-Pot, Water-Based and High-Yield Synthesis of Tetrahedral Palladium Nanocrystal Decorated Grapheme. *Nanoscale* **2013**, *5*, 8007–8014

(3) Zhu, M. Y.; Wang, C. J.; Meng, D. H.; Diao, G. W. In Situ Synthesis of Silver Nanostructures on Magnetic Fe_3O_4@C Core–Shell Nanocomposites and their Application in Catalytic Reduction Reactions. *J. Mater. Chem. A* **2013**, *1*, 2118–2125.

(4) Ma, J. X.; Yang, H. L.; Li, S. W.; Ren, R.; Li, J.; Zhang, X. Y.; Ma, J. T. Well-Dispersed Graphene-Polydopamine-Pd Hybrid with Enhanced Catalytic Performance. *RSC Adv*. **2015**, *5*, 97520–97527.

(5) Wu, M. L.; Li, Y. Y.; Yue, R.; Zhang X. D.; Huang, Y. M. Removal of Silver Nanoparticles by Mussel-Inspired Fe_3O_4@Polydopamine Core-Shell Microspheres and its Use as Efficient Catalyst for Methylene Blue Reduction. *Sci. Rep.* **2017**, *7*, 42773.

(6) Xie, Y. J.; Yan, B.; Xu, H. L.; Chen, J.; Liu, Q. X.; Deng Y. H.; Zeng, H. B. Highly Regenerable Mussel-Inspired Fe_3O_4@Polydopamine-Ag Core–Shell Microspheres as Catalyst and Adsorbent for Methylene Blue Removal. *ACS Appl. Mater. Interfaces* **2014**, *6*, 8845−8852.

(7) Banazadeh, A.; Salimi, H.; Khaleghi, M.; Shafiei-Haghighi, S. Highly Efficient Degradation of Hazardous Dyes in Aqueous Phase by Supported Palladium Nanocatalyst—A Green Approach. *J. Environ. Chem. Eng*. **2016**, *4*, 2178–2186.

(8) Vilas, V.; Philip, D.; Mathew, Facile One-Pot Synthesis of Crystalline Palladium Nanoparticles with Exceptional Catalytic and Antiradical Activities. *J. Mater. Chem. Phys*. **2016**, *170*, 1–11.

(9) Cho, K. Y.; Yeom, Y. S.; Seo, H. Y.; Kumar, P.; Lee, A. S.; Baek, K. Y.; Yoon, H. G. Ionic Block Copolymer Doped Reduced Graphene Oxide Supports with Uultra-Fine Pd Nnanoparticles: Strategic Realization of Ultra-Accelerated Nnanocatalysis. *J. Mater. Chem. A* **2015**, *3*, 20471–20476.

(10) Cui, X. L.; Zheng, Y. F.; Tian, M.; Dong, Z. P. Novel Yolk–Shell-Structured Fe_3O_4@γ-AlOOH Nanocomposite Modified with Pd Nanoparticles as a Recyclable Catalyst with Excellent Catalytic Activity. *Appl. Surf. Sci.* **2017**, *416*, 103–111.

(11) Chen, F. J.; Gong, A. S.; Zhu, M. W.; Chen, G.; Lacey, S. D.; Jiang, F.; Li, Y. F.; Wang, Y. B.; Dai, J. Q.; Yao, Y. G.; Song, J. W.; Liu, B. Y.; Fu, K.; Das, S.; Hu, L. Mesoporous, Three-Dimensional Wood Membrane Decorated with Nanoparticles for Highly Efficient Water Treatment. *ACS Nano* **2017**, *11*, 4275–4282.

(12) Kim, T.; Fu, X.; Warther, D.; Sailor, M. J. Size-Controlled Pd Nanoparticle Catalysts Prepared by Galvanic Displacement into a Porous Si-Iron Oxide Nanoparticle Host. *ACS Nano* **2017**, *11*, 2773–2784.

(13) Ncube, P.; Bingwa, N.; Baloyi H.; Meijboom, R. Catalytic Activity of Palladium and Gold Dendrimer-Encapsulated Nanoparticles for Methylene Blue Reduction: A Kinetic Analysis. *Appl. Catal. A* **2015**, *495*, 63–71.

(14) Ni, X. J.; Wu, Z. F.; Gu, X. D.; Wang, D. W.; Yang, C.; Sun, P. D.; Li, Y. X. In Situ Growth of Clean Pd Nanoparticles on Polystyrene Microspheres Assisted by Functional Reduced Graphene Oxide and Their Excellent Catalytic Properties. *Langmuir* **2017**, *33*, 8157–8164.

(15) Le, X. D.; Dong, Z. P.; Liu, Y. S.; Jin, Z. C.; Huy, T. D.; Le M.; Ma, J. T. Palladium Nanoparticles Immobilized on Core–Shell Magnetic Fibers as a Highly Efficient and Recyclable Heterogeneous Catalyst for the Reduction of 4-Nitrophenol and Suzuki Coupling Reactions. *J. Mater. Chem. A* **2014**, *2*,19696–19706.

(16) Fareghi-Alamdari, R.; Haqiqib, M. G.; Zekri, N. Immobilized Pd(0) Nanoparticles on Phosphine-Functionalized Graphene as a Highly Active Catalyst for Heck, Suzuki and *N*-arylation Reactions. *New J. Chem.* **2016**, *40*, 1287–1296.

(17) Zhang, S.; Li, J.; Gao, W.; Qu, Y. Q. Insights Into the Effects of Surface Properties of Oxides on the Catalytic Activity of Pd for C–C Coupling Reactions. *Nanoscale* **2015**, *7*, 3016–3021.

(18) Putta, C.; Sharavath, V.; Sarkara, S.; Ghosh, S. Palladium Nnanoparticles on β-Cyclodextrin Functionalised Graphene Nanosheets: A Supramolecular Based Heterogeneous Catalyst for C–C Coupling Reactions under Green Reaction Conditions. *RSC Adv*. **2015**, *5*, 6652–6660.

(19) Xia, J. W.; Fu, Y. S.; He, G. Y.; Sun, X. Q.; Wang, X. Core-Shell-Like Ni-Pd Nanoparticles Supported on Carbon Black as a Magnetically Separable Catalyst for Green Suzuki-Miyaura Coupling Reactions. *Appl. Catal. B* **2017**, *200*, 39–46.

(20) Yu, D.; Bai, J.; Wang, J. Z.; Liang, H.; Li, C. P. Assembling Formation of Highly Dispersed Pd Nanoparticles Supported 1D Carbon Fiber Electrospun with Excellent Catalytic Active and Recyclable Performance for Suzuki Reaction. *Appl. Surf. Sci.* **2017**, *399*, 185–191.

(21) Wu, L.; Yuan, B.; Liu, M. M.; Huo, H. F.; Long, Y.; Ma, J. T.; Lu, G. X. A Facile Synthesis of a Solvent-Dispersible Magnetically Recoverable Pd^0 Catalyst for the C–C Coupling Reaction. *RSC Adv*. **2016**, *6*, 56028–56034.

(22) Fu, W. Z.; Zhang, Z. Q.; Zhuang, P. Y.; Shen, J. F.; Ye, M. X. One-Pot Hydrothermal Synthesis of Magnetically Recoverable Palladium/Reduced Graphene Oxide Nanocomposites and its Catalytic Applications in Cross-Coupling Reactions. *J. Colloid Interface Sci*. **2017**, *497*, 83–92.

(23) Karami, K.; Ghasemi, M.; Naeini, N. H. Palladium Nanoparticles Supported on Polymer: An Efficient and Reusable Heterogeneous Catalyst for the Suzuki Cross-Coupling Reactions and Aerobic Oxidation of Alcohols. *Catal. Commun*. **2013**, *38*, 10–15.

(24) Zhou, H.; Wu, C. G.; Wu, Q. L.; Guo, B. X.; Liu, W. T.; Li, G. H.; Su, Q.; Mu, Y. Palladium Nanoparticles Supported on a Carbazole Functionalized Mesoporous Organic Polymer: Synthesis and Their Application as Efficient Catalysts for the Suzuki–Miyaura Cross Coupling Reaction. *Polym. Chem*. **2017**, *8*, 1488–1494.

(25) Hajipour, A. R.; Abolfathia, P.; Mohammadsaleh, F. A Click Strategy for the Immobilization of Palladium Nanoparticles onto Silica: Efficient and Recyclable Catalysts for Carbon–Carbon Bond Formation under Mild Reaction Conditions. *RSC Adv*. **2016**, *6*, 78080–78089.

(26) Gholinejad, M.; Razeghi, M.; Ghaderi, A.; Bijic, P. Palladium Supported on Phosphinite Functionalized Fe_3O_4 Nanoparticles as a New Magnetically Separable Catalyst for Suzuki–Miyaura Coupling Reactions in Aqueous Media. *Catal. Sci. Technol*. **2016**, *6*, 3117–3127.

(27) Ye, W.; Yu, J.; Zhou, Y.; Gao, D.; Wang, D.; Wang, C.; Xue, D. Green Synthesis of Pt–Au Dendrimer-Like Nanoparticles Supported on Polydopamine-Functionalized Graphene and their High Pperformance toward 4-Nitrophenol Reduction. *Appl. Catal. B* **2016**, *181*, 371–378.

(28) Lu, W.; Ning, R.; Qin, X.; Zhang, Y.; Chang, G.; Liu, S.; Luo, Y.; Sun, X. Synthesis of Au Nanoparticles Decorated Graphene Oxide Nanosheets: Noncovalent Functionalization by TWEEN 20 in Situ Reduction of Aqueous Chloroaurate Ions for Hydrazine Detection and Catalytic Reduction of 4-Nitrophenol. *J. Hazard. Mater.* **2011**, *197*, 320–326.

(29) Hareesh, K.; Joshi, R. P.; Sunitha, D. V.; Bhoraskar, V. N.; Dhole, S. D. Anchoring of Ag-Au alloy Nanoparticles on Reduced Graphene Oxide Sheets for the Reduction of 4-Nitrophenol. *Appl. Surf. Sci*. **2016**, *389*, 1050–1055.

(30) Wang, D. M.; Duan, H. C.; Lü J. H.; Lü, C. Fabrication of Thermo-Responsive Polymer Functionalized Reduced Graphene Oxide@Fe_3O_4@Au Magnetic Nanocomposites for Enhanced Catalytic Applications. *J. Mater. Chem. A* **2017**, *5*, 5088–5097.

(31) Xi, J. B.; Xiao, J. W.; Xiao, F.; Jin, Y. X.; Dong, Y.; Jing F.; Wang, S. Mussel-Inspired Functionalization of Cotton for Nano-Catalyst Support and its Application in a Fixed-bed System with High Performance. *Sci. Rep.* **2016**, *6*, 21904.

(32) Fageria, P.; Uppala, S.; Nazir, R.; Gangopadhyay, S.; Chang, C. H.; Basu, M.; Pande, S. Synthesis of Monometallic (Au and Pd) and Bimetallic (AuPd) Nanoparticles using Carbon Nitride (C_3N_4) Quantum Dots via the Photochemical Route for Nitrophenol Reduction. *Langmuir* **2016**, *32*, 10054–10064.

(33) Wu, X. D.; Lu, C. H.; Zhang, W.; Yuan, G. P.; Xiong, R.; Zhang, J. X. A Novel Reagentless Approach for Synthesizing Cellulose Nanocrystal-Supported Palladium Nanoparticles with Enhanced Catalytic Performance. *J. Mater. Chem. A* **2013**, *1*, 8645–8652.

(34) Liu, X.; Cheng, F.; Liu,Y.; Ji, H.; Chen, Y. Preparation and Characterization of Novel Thermoresponsive Gold Nanoparticles and Their Responsive Catalysis Properties. *J. Mater. Chem.* **2010**, *20*, 360–368.